HHS Public Access

Author manuscript

Cell Host Microbe. Author manuscript; available in PMC 2023 February 09.

Published in final edited form as:

Cell Host Microbe. 2022 February 09; 30(2): 163–170.e6. doi:10.1016/j.chom.2021.12.001.

Virulence factors perforate the pathogen-containing vacuole to signal efferocytosis

Hirotaka Hiyoshi[1,2], **Bevin C. English**[2], **Vladimir E. Diaz-Ochoa**[2], **Tamding Wangdi**[2,3], **Lillian F. Zhang**[2], **Miako Sakaguchi**[4], **Takeshi Haneda**[5], **Renée M. Tsolis**[2], **Andreas J. Bäumler**[2,*]

[1]Department of Bacteriology, Institute of Tropical Medicine, Nagasaki University, 1-12-4 Sakamoto, Nagasaki 852-8523, Japan

[2]Department of Medical Microbiology and Immunology, University of California at Davis, One Shields Ave, Davis CA 95616, USA

[3]Current address: BioMerieux, 595 Anglum Road, Hazelwood, MO 63042

[4]Central Laboratory, Institute of Tropical Medicine, Nagasaki University, 1-12-4 Sakamoto, Nagasaki 852-8523, Japan

[5]Laboratory of Microbiology, School of Pharmacy, Kitasato University, 5-9-1, Shirokane, Minato-ku, Tokyo 108-8641, Japan

SUMMARY

Intracellular pathogens commonly reside within macrophages to find shelter from humoral defenses, but host cell death can expose them to the extracellular milieu. We find intracellular pathogens solve this dilemma by using virulence factors to generate a complement-dependent find-me signal that initiates uptake by a new phagocyte though efferocytosis. During macrophage death, *Salmonella* uses a type III secretion system to perforate the membrane of the pathogen-containing vacuole (PCV), thereby triggering complement deposition on bacteria entrapped in pore-induced intracellular traps (PITs). In turn, complement activation signals neutrophil efferocytosis, a process that shelters intracellular bacteria from the respiratory burst. Similarly, *Brucella* employs its type IV secretion system to perforate the PCV membrane, which induces complement deposition on bacteria entrapped in PITs. Collectively, this work identifies virulence factor-induced perforation of the PCV as a strategy of intracellular pathogens to generate a find-me signal for efferocytosis.

[*]Lead contact and correspondence: ajbaumler@ucdavis.edu.

AUTHOR CONTRIBUTIONS

Conceptualization, H.H., R.M.T. and A.J.B. Methodology, H.H., B.C.E., V.E.D.-O., T.W., M.S., L.F.Z., T.H., R.M.T. and A.J.B.; Investigation, H.H., B.C.E., V.E.D.-O., T.W., M.S., L.F.Z., T.H., R.M.T. and A.J.B.; Resources, A.J.B.. Funding Acquisition, H.H., L.F.Z., R.M.T. and A.J.B.; Writing – Original Draft, H.H., R.M.T. and A.J.B.; Writing – Review & Editing, H.H., R.M.T. and A.J.B.; Supervision, H.H., R.M.T. and A.J.B.

DECLARATION OF INTERESTS

The authors declare no competing interests

eTOC blurb

Hirotaka et al. find that *Salmonella* uses T3SS-2 to perforate the phagosome of macrophages, thereby generating a complement-dependent find-me signal for efferocytosis by neutrophils. Efferocytosis of *Salmonella* entrapped in dying macrophages shelters the pathogen from the neutrophil respiratory burst, thereby enabling the pathogen to evade neutrophil-mediated host control.

Graphical Abstract

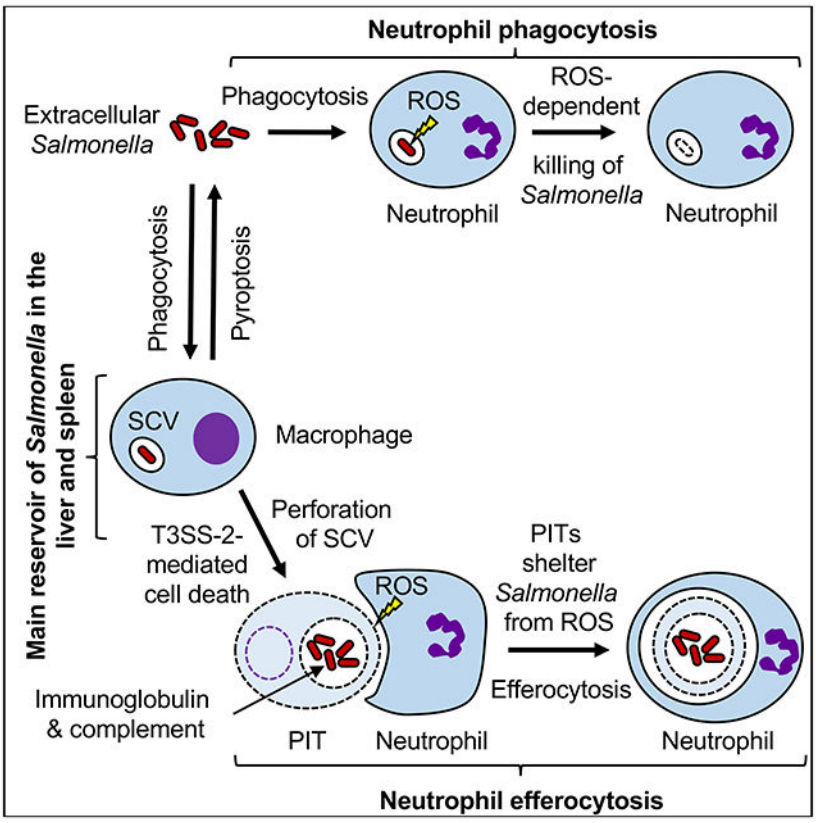

INTRODUCTION

Macrophages are a popular replicative niche for intracellular pathogens, such as *Salmonella enterica* serovar Typhimurium (*STm*) or *Brucella abortus* (*BA*). These pathogens reside predominantly in a PCV within macrophages of the liver and spleen (Atluri et al., 2011; Richter-Dahlfors et al., 1997), a niche that shelters them from humoral defenses. However, growth in tissue involves the formation of new infection foci (Grant et al., 2012), suggesting that pathogens must transit to new host cells over time, thereby risking exposure to the extracellular milieu.

BA requires a type IV secretion system (T4SS) for growth in the liver and spleen of mice (Hong et al., 2000). The T4SS functions in the translocation of proteins, termed effectors, into the macrophage cytosol (de Barsy et al., 2011; de Jong et al., 2008; Marchesini et

al., 2011; Myeni et al., 2013), which can result in cell death (Li et al., 2017; Pei et al., 2008; Tian et al., 2020). Similarly, growth of *STm* in the liver and spleen of mice is associated with death of infected macrophages (Richter-Dahlfors et al., 1997). *STm* induces macrophage death *in vitro* by deploying two type III secretion systems, termed T3SS-1 and T3SS-2 (Monack et al., 1996; van der Velden et al., 2000). T3SS-1 and T3SS-2 function in the translocation of effectors into the host cell cytosol (LaRock et al., 2015). Perhaps inadvertently, T3SS-1 also translocates flagellin (FliC), the main subunit of bacterial flagella, into the host cell cytosol (Sun et al., 2007), which triggers pyroptosis (Cookson and Brennan, 2001), a Caspase-1-mediated form of cell death associated with pore-induced lysis (Fink and Cookson, 2019; Franchi et al., 2006; Miao et al., 2006). However, *STm* shuts off flagellin synthesis in the liver and spleen of mice (Cummings et al., 2006), thereby evading pyroptosis.

Whereas flagellin synthesis is turned off in the murine spleen (Cummings et al., 2006), a *STm* strain genetically engineered to synthesize flagellin in splenic tissue is cleared by neutrophils (Jorgensen et al., 2016), suggesting that an unphysiological induction of pyroptosis is detrimental to the pathogen. Paradoxically, although T3SS-2 can induce a flagellin-independent form of macrophage cell death (Matsuda et al., 2019), this virulence factor is required for *STm* growth in tissue (Hensel et al., 1995). It remains unclear why flagellin-dependent cell death is detrimental for *STm* (Jorgensen et al., 2016), whereas flagellin-independent cell death induced by T3SS-2 (Matsuda et al., 2019) is beneficial during growth in tissue (Grant et al., 2012). The goal of this study was to resolve this apparent paradox.

RESULTS

STm uses T3SS-2 to overcome neutrophil-mediated defenses *in vivo*

T3SS-2-deficient *STm* mutants replicate normally in macrophages *in vivo* but are unable to evade phagocyte NADPH oxidase-dependent killing during dissemination to new foci of infection (Grant et al., 2012; Vazquez-Torres et al., 2000). We thus hypothesized that T3SS-2-deficient *STm* mutants are exposed to NADPH oxidase-dependent killing mechanisms of phagocytes when bacteria transit from a deceased host cell to an extracellular location. Since NADPH oxidase-dependent control of *STm* growth in tissue is mainly attributed to neutrophils and inflammatory monocytes (Burton et al., 2014), we determined whether an antibody-mediated depletion of either cell type would rescue growth of a T3SS-2-deficient (*spiB*) mutant. Treatment of mice with an anti-CCR2 antibody resulted in depletion of inflammatory monocytes (Fig. 1A) but did not increase the fitness of the *spiB* mutant compared to the *STm* wild type (Fig. 1B and S1A). In contrast, depletion of neutrophils with anti-Ly6G antibody (Fig. 1C) partially rescued growth of a *spiB* mutant (Fig. 1D, 1E, S1B and S1C), but not a mutant lacking *aroA* (Fig 1F and 1G), a gene required for intracellular growth within macrophages *in vivo* (Grant et al., 2012). Thus, T3SS-2 functions in evading neutrophil-mediated host control subsequent to *STm* growth within macrophages.

T3SS-2 perforates the *Salmonella*-containing vacuole (SCV) to activate complement

To investigate whether extracellular bacteria use T3SS-2 to evade killing by neutrophils, we infected primary neutrophils with *STm* wild type or a *spiB* mutant. Wild type and a *spiB* mutant exhibited similar sensitivity to neutrophil-mediated killing, which could be inhibited by addition of the NADPH-oxidase inhibitor diphenyleneiodonium chloride (DPI) (Fig 2A). Thus, *STm* did not evade the neutrophil respiratory burst in a T3SS-2-dependent fashion, which was consistent with a proposed role of neutrophils in preventing extracellular replication of *STm* in the liver of mice (Conlan, 1996).

Next, we investigated whether the role of the T3SS-2 in evading the neutrophil respiratory burst could be modeled using *STm*-infected macrophages *in vitro*. To this end, murine macrophage-like (RAW264.7) cells were infected with *STm* and cultured for 23 hours, followed by the addition of primary murine neutrophils in 10% normal mouse serum. Numbers of the *STm* wild type increased between 3 hours and 21 hours after the addition of neutrophils, which required a functional T3SS-2 (Fig 2B). Notably, neutrophils migrated towards *STm*-containing macrophages, but not towards macrophages infected with a *spiB* mutant (Fig. 2C), suggesting that T3SS-2 was required for generating a chemotactic signal. This chemotactic signal resulted in the internalization of wild-type *STm* by neutrophils (Fig. 2D), which was not observed for a *spiB* mutant.

STm-induced neutrophil chemotaxis requires complement activation (Wangdi et al., 2014). We thus visualized complement component (C) 3 deposition during infection of macrophages. Interestingly, C3 staining that colocalized with bacteria was observed in macrophages as early as 12 hours after infection with the *STm* wild type, whereas no C3 staining was detected in macrophages containing a *spiB* mutant (Fig. 2E, 2F, S2A and S2B), even after allowing the infection to progress for 48 hours (Fig. S2C).

We next investigated whether C3 deposition was a consequence of pore-induced macrophage cell death triggered by T3SS-1 or T3SS-2. *STm* infection of macrophages increased cytoplasmic membrane permeability as indicated by positive propidium iodide staining (Fig. S2D). Release of the intracellular enzyme lactate dehydrogenase (LDH) was markedly reduced 24 hours after infection of macrophages with a *STm* strain lacking both T3SS-1 and T3SS-2 (*invA spiB* mutant) (Fig. 2G). However, genetic ablation of T3SS-1 (*invA* mutant) did not prevent C3 deposition (Fig. 2E and 2F), despite the fact that bacteria carrying a functional T3SS-1 (*spiB* mutant) triggered greater LDH release than an isogenic mutant lacking this virulence factor (*invA spiB* mutant) (Fig. 2G).

Since T3SS-1 and T3SS-2 both induce LDH release (Monack et al., 1996; van der Velden et al., 2000), but only T3SS-2 triggered C3 deposition on intracellular bacteria (Fig. 2E and 2F), we hypothesized that pore-induced cell death was not sufficient for complement activation. We thus investigated whether T3SS-2 permeabilizes the SCV to trigger C3 deposition on intracellular bacteria. Permeabilization of the vacuolar membrane of macrophages with the detergent saponin (Meunier and Broz, 2015) restored C3 deposition on the *spiB* mutant (Fig. 3A). Bacteria localized in an intact vacuolar compartment are susceptible to killing by the lysosomotropic agent chloroquine, but bacteria that are cytosolic are chloroquine-resistant (Knodler et al., 2014). Consistent with a T3SS-2-

mediated permeabilization of the vacuolar membrane, macrophages infected with the *STm* wild type contained a larger fraction of chloroquine-resistant bacteria (Fig. 3B) and a larger fraction of intact bacteria detected by electron microscopy (Fig. 3C and 3D) compared to macrophages infected with the *spiB* mutant. Galectin-8 monitors endo-lysosomal integrity and detects bacterial invasion of the cytosol by binding host glycans exposed on damaged SCVs (Thurston et al., 2012). Galactin-8 localized to bacteria in macrophages infected with the *STm* wild type, but not to bacteria in macrophages infected with a *spiB* mutant (Fig. S2E). Complement activation by *STm* proceeds through the classical pathway, which is induced when natural IgM binds the O-antigen of lipopolysaccharide (LPS) on the bacterial surface (Hiyoshi et al., 2018). We thus determined whether binding of antibodies to LPS on intracellular bacteria was observed after permeabilization of the macrophage plasma membrane or permeabilization of the vacuolar membrane. Digitonin treatment, which selectively permeabilizes the cholesterol-rich plasma membrane (Meunier and Broz, 2015), did not result in LPS labeling of the *spiB* mutant within infected macrophages (Fig. 3E). In contrast, treatment with saponin, which permeabilizes vacuolar membranes (Meunier and Broz, 2015), resulted in LPS labeling of the *spiB* mutant within infected macrophages (Fig. 3E). Thus, T3SS-2 impairs endo-lysosomal integrity of the SCV to trigger complement-deposition.

Complement-induced efferocytosis of PITs limits ROS-dependent killing

We next wanted to determine whether complement deposition on bacteria entrapped in PITs triggers neutrophil efferocytosis. Addition of neutrophils to PITs containing the *STm* wild type triggered a respiratory burst, as measured by a luminol-based bioassay for generation of reactive oxygen species (ROS) (Fig. 4A and 4B). Notably, PITs containing a *spiB* mutant did not elicit ROS generation from neutrophils. The neutrophil respiratory burst was no longer observed when the assay was repeated in the absence of normal mouse serum (Fig. 4C) and was significantly reduced after addition of the complement inhibitor futhan (6-amidino-2-naphthyl p-guanidinobenzoate dimethanesulfonate) (Ikari et al., 1983) (Fig. 4D) or when the experiment was repeated with neutrophils from mice lacking the receptor for C5a (*C5aR1*-deficient mice) (Fig. 4E), a neutrophil chemoattractant generated during the complement cascade. These results were consistent with the idea that T3SS-2-dependent complement activation by bacteria entrapped in PITs (Fig. 2E, 2F, 4C, 4D and 4E) induced a neutrophil respiratory burst during efferocytosis (Fig. 2C, 2D, 4A and 4B). Paradoxically, this T3SS-2-dependent induction of the neutrophil respiratory burst resulted in enhanced bacterial recovery (Fig. 2B), suggesting that neutrophil efferocytosis was beneficial for the pathogen despite triggering ROS production.

We hypothesized that PITs might shelter entrapped bacteria from ROS generated during the respiratory burst of neutrophils during efferocytosis, whereas extracellular bacteria would remain sensitive to ROS exposure during phagocytosis. To visualize bacterial exposure to ROS during phagocytosis or efferocytosis, we generated a *STm* strain expressing green fluorescent protein (GFP) under control of the *katG* promoter, which rendered GFP synthesis responsive to hydrogen peroxide exposure (Fig S3A). Notably, phagocytosis of extracellular bacteria by neutrophils resulted in ROS production (Fig. 4F and 4G) and GFP synthesis (Fig. 4H). However, despite ROS production during neutrophil efferocytosis of PITs (Fig. 4A),

GFP synthesis was not detected in bacteria located within neutrophils after efferocytosis (Fig. 4H). To further corroborate the idea that PITs shelter bacteria from ROS exposure, we compared expression of hydrogen peroxide-inducible *STm* genes (*katG* and *oxyR*) (Fig. S3B and S3C) during neutrophil phagocytosis or efferocytosis. A marked induction of *katG* and *oxyR* expression was observed after phagocytosis, but this response was absent during efferocytosis (Fig. 4I). Finally, we determined whether inhibition of NADPH-oxidase using DPI would improve recovery of *STm* in our neutrophil efferocytosis assay. Notably, inhibition of NADPH-oxidase activity did not improve bacterial recovery during efferocytosis (Fig S3D), which was in marked contrast to the increase in *STm* recovery triggered by DPI treatment during phagocytosis (Fig. 2A). Thus, T3SS-2-induced neutrophil efferocytosis enables *STm* entrapped in PITs to evade the respiratory burst, which explains why neutrophils become a 'safe-site' for the pathogen in the spleen (Dunlap et al., 1992).

The T4SS perforates the *Brucella*-containing vacuole (BCV) to generate a find-me signal

The intracellular pathogen *BA* uses a type IV secretion system (T4SS) encoded by the *virB* operon to survive in macrophages during chronic infection (Hong et al., 2000), but this virulence factor is not required prior to the onset of adaptive immune responses (Rolan and Tsolis, 2007). *BA* LPS displays an O-antigen that prevents opsonization with naïve murine serum (Barquero-Calvo et al., 2007), however the development of an antibody response during chronic *BA* infection overcomes complement evasion by the O-antigen. Thus, we opsonization wild-type *BA* with anti-*Brucella* immune serum to model the chronic phase of infection, when the T4SS is required for growth in tissue (Rolan and Tsolis, 2007).

Macrophages infected with opsonized *BA* underwent cell death, which could be prevented by genetic ablation of the T4SS (*virB2* mutant) (Fig. S4A). Interestingly, C3 staining that colocalized with bacteria was observed in a fraction of macrophages infected with the *BA* wild type or a complemented *virB2* mutant, whereas no C3 staining was detected in macrophages containing a *virB2* mutant, even when cells were infected with a 5-fold higher multiplicity of infection (Fig. S4B). The addition of neutrophils to PITs containing the *BA* wild type triggered efferocytosis characterized by a respiratory burst, but addition of neutrophils to PITs containing a *virB2* mutant did not elicit this response (Fig. S4C and S4D). Furthermore, a serum-dependent respiratory burst was no longer observed when the assay was repeated with neutrophils from *C5aR1*-deficient mice (Fig. S4E). Thus, the T4SS perforates the BCV to generate a complement-dependent find-me signal for efferocytosis.

DISCUSSION

The picture emerging from these studies is that the type of host cell death induced during infection governs the outcome of host pathogen interaction. Host cells can detect the translocation of flagellin into the host cell cytosol as a "pattern of pathogenesis" (Vance et al., 2009) to induce pyroptosis (Franchi et al., 2006; Miao et al., 2006), a type of host cell death that releases bacteria into the extracellular space where they are vulnerable to clearance by neutrophils through phagocytosis. Consistent with this idea, an unphysiological induction of flagellin synthesis in *STm* or *B. melintensis* results in pathogen clearance from the spleen by pyroptosis (Jorgensen et al., 2016; Terwagne et al., 2013). Pathogens

can avoid pyroptosis by limiting flagellin synthesis in tissue (Cummings et al., 2006), but in the absence of flagellin-induced cell death they require alternate mechanisms to ensure transition between host cells.

Our results suggest that *STm* and *BA* solve this dilemma by using their virulence factors to trigger a form of cell death that leads to the perforation of the PCV to trigger efferocytosis. The process of PIT efferocytosis likely requires eat-me signals, such as exposure of phosphatidyl serine at the cell surface (Fadok et al., 2001). However, eat-me signals alone were not sufficient to induce efferocytosis, because T3SS-1 mediated pyroptosis induced pore-induced cell death, but not efferocytosis of *STm*-containing PITs by neutrophils. Instead, the latter process required perforation of the PCV by T3SS-2, which enabled *STm* entrapped in PITs to activate complement, thereby generating a find-me signal to attract neutrophils.

In contrast to phagocytosis, neutrophil-mediated efferocytosis of PITs shelters the entrapped pathogen from ROS exposure. How do PITs shelter the pathogen from ROS? One possible mechanism is localized ROS production by neutrophils, resulting in dilution in a gradient and detoxification by superoxide dismutase, catalase and glutathione peroxidase activity, as ROS diffuses through the PIT (Herb et al., 2021). As a result, a virulence factor-mediated perforation of the PCV enables intracellular pathogens to evade pyroptosis-mediated host control during their transition between host cells.

STAR METHODS

Resource Availability

Lead Contact—Further information and requests for resources and reagents should be directed to and will be fulfilled by the Lead Contact, Andreas J. Bäumler (ajbaumler@ucdavis.edu).

Materials Availability—The study did not create new unique reagents. Further information and requests for resources and reagents should be directed to and will be fulfilled by the Lead Contact.

Data and Code Availability

- The study did not create large data sets that required deposition in a public data base. Microscopy data reported in this paper will be shared by the lead contact upon request.
- The study did not create original code.
- Any additional information required to reanalyze the data reported in this paper is available from the lead contact upon request.

Experimental model and subject details

Animal experiments—The Institutional Animal Care and Use Committee at the University of California, Davis, approved all animal experiments. Female 7 to 8 week-old C57BL/6J (stock no. 000664) mice and congenic C5aR-deficient mice (B6.129S4(C)-

C5ar1^{tm1Cge}/BaoluJ) (stock no. 033903) were purchased from the Jackson Laboratories. Prior to transport, mice at Jackson were fed LabDiet 5K52 formulation (6% fat). Upon arrival, mice from each cohort were randomly assigned into individually ventilated cages on one rack at a housing density of 3 to 4 animals per cage and allowed to acclimate in our vivarium for at least a week undisturbed. Feed was switched to irradiated TEKLAD GLOBAL 18% protein rodent diet 2918 (Envigo) and no breeding was performed. 70% ethanol was used to disinfect surfaces and gloves between groups. Clean (but not sterile) paper towels were utilized for fecal sample collections. Numbers of animals used in each group are indicated on each graph or in the figure legends.

Bacterial strains and culture conditions—Bacterial strains and Plasmids used in this study are presented in Table S1. *S.* Typhimurium strains were routinely cultured with aeration at 37°C in Luria-Bertani (LB) broth (10 g tryptone, 5 g yeast extract, and 10 g NaCl per liter) or on LB agar plates unless indicated otherwise. *B. abortus* was cultured on blood agar plates (UC Davis Veterinary Medicine Biological Media Services) for 3 days at 37°C with 5% CO_2. Antibiotics were added as appropriate. For all *in vitro* assays, *S.* Typhimurium strains were routinely prepared by inoculating LB broth with an overnight culture, followed by culturing for approximately 3 hours until an OD_{600} of 1.0 was reached. *B. abortus* was cultured overnight at 37°C with aeration in tryptic soy broth (TSB; BD Difco™) then subcultured in acidic EGY (pH 5.5) for 4 hours at 37°C with aeration.

Cell lines and primary cell cultures—RAW264.7 murine macrophage-like cells (TIB-71; ATCC) were cultured in RPMI1640 supplemented with 10% fetal bovine serum (FBS) and GlutaMAX™ Supplement (Gibco, #35050061) at 37°C in 5% CO_2.

Primary murine neutrophils were isolated from bone marrow (BM) of murine femurs of female 7 to 8 week-old C57BL/6J (stock no. 000664) mice and congenic C5aR-deficient mice (B6.129S4(C)-*C5ar1*^{tm1Cge}/BaoluJ) (stock no. 033903) by using EasySep™ Mouse Neutrophil Enrichment Kit (StemCell Technologies) according to the manufacturer's instruction.

To generate bone marrow-derived macrophages (BMDMs), bone marrow cells from C57BL/6J (stock no. 000664) mice were differentiated by RPMI1640 supplemented with 10% FBS, 30% L929 cell supernatant, and GlutaMAX™ at 37°C in 5% CO_2 for 7 days.

Method details

Depletion of neutrophils and inflammatory monocytes—To deplete neutrophils, C57BL/6J mice were injected with anti-Ly-6G antibody (1A8; Bio X Cell) intraperitoneally twice (one day before and one day after *S.* Typhimurium infection). An isotype matched antibody (2A3) was injected into mice of the isotype control group.

To deplete inflammatory monocytes, mice received three injections of anti-CCR2 antibody (MC-21) (Mack et al., 2001) intraperitoneally (one day before, the day of and one day after *S.* Typhimurium infection). An isotype matched antibody (LTF-2) was injected into mice of the isotype control group.

Depletion of neutrophils and inflammatory monocytes was assessed by flow cytometry. Spleens were isolated and suspensions of splenocytes were stained by Live/Dead Aqua dye, and CD3, NK1.1, B220, CD11b, Gr-1, and CD115 antibodies, and fixed by BD Cytofix™ Fixation buffer (Becton Dickinson). Stained cells were analyzed by LSR II (Becton Dickinson) and FlowJo™ (Becton Dickinson). The fractions of neutrophil (Gr-1^{hi}, $CD115^{-}$) and inflammatory monocyte (Gr-1^{hi}, $CD115^{+}$) in life, single cell suspensions of $CD11b^{+}$, $CD3^{-}$, $NK1.1^{-}$, $B220^{-}$ cells were gated out as described previously (Zhang et al., 2009).

S. Typhimurium infection of mice—*S.* Typhimurium strains were grown overnight and 10^5 colony-forming units (cfu) of a 1:1 mixture of the indicated *S.* Typhimurium strains suspended in 100 μL phosphate buffed saline (PBS) were injected into C57BL/6J mice intraperitoneally. Two days after infection, cfu of each strain were determined in homogenates of the liver and spleen by spreading serial ten-fold dilutions on agar plates containing the appropriate antibiotics and the competitive index (CI) (ratio of wild type/mutant) was calculated.

Efferocytosis assay—One day before infection, 2×10^5 RAW264.7 murine macrophage-like cells were seeded in 6-well plates and cultured in RPMI1640 supplemented with 10% fetal bovine serum (FBS) and GlutaMAX™ Supplement (Gibco, #35050061), referred to hereafter as RPMI1640S medium, at 37°C in 5% CO_2. Primary murine neutrophils were isolated from bone marrow (BM) of murine femurs by using EasySep™ Mouse Neutrophil Enrichment Kit (StemCell Technologies). For infection, *S.* Typhimurium strains were opsonized by incubation in 20% normal mouse serum (NMS) for 30 min at room temperature, and RAW264.7 cells were infected with 5×10^6 cfu opsonized *S.* Typhimurium (multiplicity of infection, MOI =10), immediately centrifuged at 250 × g for 5 minutes, and incubated in an incubator (37°C, 5% CO_2) for 30 minutes to allow RAW264.7 cells to take up bacteria. Then, 100 μg/mL gentamicin was added for 30 minutes to kill extracellular bacteria, followed by incubation with 10 μg/mL gentamicin for the duration of the experiment. 23 hours after infection, infected RAW264.7 cells were opsonized with 10% normal murine serum (NMS) for 30 minutes and cells were collected and counted. In some experiments, normal mouse serum was incubated with 2 mg/mL Futhan (Ikari et al., 1983) at 37°C for 30 min prior to opsonizing infected RAW264.7 cells. 1×10^5 infected RAW264.7 cells and 1×10^5 murine primary neutrophil or sterile medium (mock group) were added to a well in a 24-well plate and incubated (37°C, 5% CO_2) to allow efferocytosis to occur. In some experiments, primary murine neutrophils were treated with 5 μM NADPH-oxidase inhibitor (diphenyleneiodonium chloride, DPI) for 30 minutes before administration. 3 hours and 21 hours after adding neutrophils, bacteria were recovered from RAW264.7 cells (mock group) or the mixture of RAW264.7 cells and neutrophils (efferocytosis group) by lysis with prechilled water. Serial ten-fold dilutions were spread on LB plates and survival and replication of *S.* Typhimurium during neutrophil efferocytosis was assessed by comparing cfu recovered at 21 hours and at 3 hours after adding neutrophils.

To visualize neutrophil recruitment to infected RAW264.7 cells, 2×10^5 RAW264.7 murine macrophage-like cells were infected with 2×10^6 cfu of the indicated GFP-labeled *S.*

Typhimurium strains (MOI =10). The plate was centrifuged at 250 × g for 5 minutes and incubated (37°C, 5% CO_2) for 30 minutes to allow for uptake of bacteria. Cells were treated for 30 minutes with 100 μg/mL gentamicin to kill extracellular bacteria and the gentamicin concentration was reduced to 10 μg/mL for the remainder of the experiment. 23 hours after infection, infected macrophages were incubated with 10% NMS for 30 minutes and then cells were collected and counted. 4×10^5 infected macrophages were added to 2×10^5 primary murine neutrophils (With neutrophils) or remained untreated (Mock) and were incubated for 4 hours (37°C, 5% CO_2). Cells were then fixed with 4% paraformaldehyde and murine neutrophils and macrophages were strained by anti-Ly-6G antibody and anti-CD14 antibody, respectively. DNA was counter stained with Hoechst 33342 and the neutrophil recruitment was visualized by fluorescence microscopy.

Phagocytosis assay—Primary murine neutrophils were isolated from bone marrow using EasySep™ Mouse Neutrophil Enrichment Kit (StemCell Technologies). Before infection, primary murine neutrophils were treated with 5 μM NADPH-oxidase inhibitor (diphenyleneiodonium chloride, DPI) for 30 minutes or remained untreated, and 5×10^6 opsonized bacteria were added to 5×10^5 primary murine neutrophils (MOI =10 unless indicated otherwise) in a 24-well plate. The plate was centrifuged at 250 × g for 5 minutes and incubated (37°C, 5% CO_2) for 30 minutes to allow neutrophils to take up bacteria. After the incubation, 100 μg/mL gentamicin was added to kill extracellular bacteria. 2 hours after infection, all neutrophils were washed with PBS, lysed by incubation with prechilled water for 15 minutes and serial ten-fold dilutions were spread on LB plates to enumerate cfu.

Detection of C3 deposition—One day before *S.* Typhimurium infection, 1×10^5 RAW264.7 murine macrophage-like cells were seeded on coverslips in 24-well plates and cultured in RPMI1640S medium at 37°C in 5% CO_2. For *Brucella* infection, 2×10^5 bone marrow-derived macrophages (BMDMs) were seeded. For infection, GFP-labeled *S.* Typhimurium strains were opsonized with normal mouse serum and RAW264.7 cells were infected with 2×10^6 cfu opsonized bacteria (MOI =10). GFP-labeled *B. abortus* strains were opsonized with *Brucella* immune mouse serum and BMDMs were infected with 2×10^7 cfu opsonized bacteria (MOI =100), unless indicated otherwise. The plates were centrifuged at 250 × g for 5 minutes and incubated (37°C, 5% CO_2) for 30 minutes to allow bacteria to be taken up. Next, cells were treated with 100 μg/mL gentamicin (*Salmonella*) or 50 ug/mL gentamicin (*Brucella*) for 30 minutes to kill extracellular bacteria and the concentration of gentamicin was subsequently reduced to 10 μg/mL for *S.* Typhimurium or removed for *B. abortus* for the remainder of the experiment. At indicated time points up to 24 hours after infection, cells were washed in PBS and incubated (37°C, 5% CO_2) in 10% NMS (*Salmonella*) or 10% *B. abortus* immunized murine serum (*Brucella*) for 30 minutes. For experiments that required permeabilization of the plasma membrane, cells were treated with 0.1% saponin before adding NMS. Cells were then fixed in 4% paraformaldehyde (PFA). Deposition of murine complement component 3 (C3) was detected by staining with anti-murine C3 antibody and cells were counterstained with Hoechst 33342. After staining, cells were mounted in antifade mounting media and then analyzed under a fluorescence microscope (ZEISS, Axio Observer or Keyence, all-in-one BZ-X700). To quantify a level of bacteria opsonized with C3, around 20 images were acquired from each infection group

and MCC (Manders' Colocalization Coefficient) was determined by analyzing images using EzColocalization, a plugin of ImageJ (Fiji) (Stauffer et al., 2018).

Chloroquine resistance assay—A method to determine chloroquine resistance of intracellular *S.* Typhimurium described previously (Knodler et al., 2014) was modified as follows. RAW264.7 murine macrophage-like cells (2×10^5 cells/well) were infected with 2×10^6 cfu of the indicated *S.* Typhimurium strains (MOI=10) as described above and incubated (37°C, 5% CO_2) for 30 minutes to allow bacteria to be taken up. Extracellular bacteria were killed by a 1-hour incubation in 100 μg/mL gentamicin and the concentration of gentamicin was subsequently reduced to 10 μg/mL for the remainder of the experiment. 2 hours before collecting samples (i.e. 1 hour and 21 hours after infection), cell were either treated with sterile medium (mock-treated) or treated with 500 μM chloroquine (chloroquine-treated) to kill intracellular bacteria located in an intact SCV. After 2 hours, *S.* Typhimurium cfu were enumerated by spreading serial ten-fold dilutions on LB agar plates. Chloroquine-resistant *S.* Typhimurium (i.e. cfu recovered from chloroquine-treated wells) were expressed as fraction of total intracellular bacteria (i.e. cfu recovered from mock-treated wells).

Permeabilization of the plasma membrane with digitonin.—A method for antibody-mediated detection of cytosolic *S.* Typhimurium using permeabilization of the plasma membrane with digitonin (Meunier and Broz, 2015) was modified as described below. In brief, 1×10^5 RAW264.7 murine macrophage-like cells were seeded on coverslips in 24-well plates and cultured in RPMI1640S medium (37°C, 5% CO_2). For infection, GFP-labeled S. Typhimurium strains were opsonized and RAW264.7 cells were infected with 2×10^6 cfu opsonized bacteria (MOI =10). The slides were centrifuged at 250 × g for 5 minutes and incubated (37°C, 5% CO_2) for 30 minutes to allow bacteria to be taken up. Next, cells were treated with 100 μg/mL gentamicin for 30 minutes to kill extracellular bacteria and the concentration of gentamicin was subsequently reduced to 10 μg/mL for the remainder of the experiment. 23 hours after infection, washed RAW264.7 cells were treated with 50 μg/mL digitonin for exactly 1 minute to permeabilize only the cytoplasmic membrane or remained untreated. Cells were washed immediately with PBS 3 times. For experiments that required permeabilization of the plasma membrane, cells were treated with 0.1% saponin. Cells were then fixed in 4% paraformaldehyde and probed by anti-LPS antibody to visualize *S.* Typhimurium. Hoechst 33342 was used to counter staining of DNA. After staining, cells were mounted in antifade mounting media and then analyzed under a fluorescence microscope (ZEISS, Axio Observer).

Detection of reactive oxygen species (ROS)—The luminol-based chemiluminescence assay for the detection of ROS during neutrophil phagocytosis of *S.* Typhimurium has been described previously (Hiyoshi et al., 2018). For monitoring ROS production during efferocytosis, 2×10^5 RAW264.7 murine macrophage-like cells were infected with *S.* Typhimurium (MOI = 10) as described above. For *Brucella* infection, 1×10^6 BMDMs per well in 6-well plates were infected with *B. abortus* strains as described above at the indicated MOIs. 23 hours after infection, infected macrophages were opsonized by adding 10% normal murine serum (NMS), 10% *B. abortus* immune serum or PBS (mock

control) for 30 minutes, and then cells were collected and counted. Primary neutrophils were treated with 1 mM luminol, and basal levels of ROS production was monitored for 5 min using a plate reader (Molecular Devices, FilterMax™ F3; or Promega, GloMax™ Explorer). RAW264.7 cells infected with *S.* Typhimurium strains or BMDMs infected with *B. abortus* were then added to neutrophils and ROS production was monitored every 2 minutes for 2 hours or 3 hours, respectively, using a plate reader.

Galection-8 localization—To visualize the damaged SCV membrane, RAW264.7 cell line stably expressing gfp-galectin-8 fusion protein was generated by transfecting a plasmid contained galectin-8 tagged N-GFPSpark (SinoBio) by Xfect™ Transfection Reagent (Clontech) and screening by Hygromycin.

One day before infection, 1×10^5 gfp-galectin-8 expressing RAW264.7 cells were seeded on coverslips in 24-well plates and cultured in RPMI1640S medium at 37°C in 5% CO_2. For infection, mCherry-labeled *S.* Typhimurium strains were opsonized with normal mouse serum and RAW264.7 cells were infected with 2×10^6 cfu opsonized bacteria (MOI=10). The plates were centrifuged at 250 × g for 5 minutes and incubated (37°C, 5% CO_2) for 30 minutes to allow bacteria to be taken up. Next, cells were treated with 100 μg/mL gentamicin for 30 minutes to kill extracellular bacteria and the concentration of gentamicin was subsequently reduced to 10 μg/mL. 16 hours after infection, cells were then fixed in 4% paraformaldehyde (PFA) and counterstained with Hoechst 33342. After staining, cells were mounted in antifade mounting media and then analyzed under a fluorescence microscope (Keyence, all-in-one BZ-X700).

Propidium iodide staining—To visualized perforated plasma membrane on the macrophages infected with *S.* Typhimurium, propidium iodide (PI) staining was performed. One day before infection, 1×10^5 RAW264.7 cells were seeded on coverslips in 24-well plates and cultured in RPMI1640S medium at 37°C in 5% CO_2. For infection, GFP-labeled *S.* Typhimurium strains were opsonized with normal mouse serum and RAW264.7 cells were infected with 2×10^6 cfu opsonized bacteria (MOI =10). The plates were centrifuged at 250 × g for 5 minutes and incubated (37°C, 5% CO_2) for 30 minutes to allow bacteria to be taken up. Next, cells were treated with 100 μg/mL gentamicin for 30 minutes to kill extracellular bacteria and the concentration of gentamicin was subsequently reduced to 10 μg/mL. 18 hours after infection, cells were incubated with 15 mM PI for 15 minutes at RT and then fixed in 4% paraformaldehyde (PFA) and counterstained with Hoechst 33342. As a positive control, uninfected cells were treated with 0.001% Trition-X100 for 5 minutes before staining by PI. After staining, cells were mounted in antifade mounting media and then analyzed under a fluorescence microscope (ZEISS, Axio Observer).

Transmission electron microscopy—RAW264.7 murine macrophage-like cells (1×10^7 cells/well) were infected with 2×10^9 cfu of the indicated *S.* Typhimurium strains (MOI=200) as described above and incubated (37°C, 5% CO_2) for 30 minutes to allow bacteria to be taken up. Extracellular bacteria were killed by a 1-hour incubation in 100 μg/mL gentamicin and the concentration of gentamicin was subsequently reduced to 10 μg/mL for the remainder of the experiment. 21 hours after infection, cells were either treated with sterile medium (mock-treated) or treated with 500 μM chloroquine (chloroquine-treated) to

kill intracellular bacteria located in an intact SCV. After 2 hours, cells were fixed with 2% glutaraldehyde in 0.1 M sodium cacodylate buffer containing 1 mM $CaCl_2$ and 1 mM $MgCl_2$ (cacodylate buffer, pH 7.4) for 60 min at 4°C. The samples were rinsed with cacodylate buffer, and then post-fixed with 1% OsO_4 in cacodylate buffer for 60 min at 4°C. They were then washed twice with cacodylate buffer, and dehydrated in graded series of ethanol (50%, 70%, 80%, and 90%) for 5 min each at 4°C and acetone (90%, 95%, 99.5%) for 5 min each at room temperature. After further dehydration with absolute acetone for 40 min and absolute propylene oxide for 10 min at room temperature, the samples were infiltrated with 2:3 mixture of absolute propylene oxide and Quetol 651 epoxy resin (Nisshin EM, Tokyo, Japan) for overnight at room temperature. They were then embedded with 100% epoxy resin in beam capsules, and polymerized for 3 days at 60°C. The resin-embedded samples were trimmed and sectioned using a diamond knife (Diatome, Nidau, Switzerland) on an ultramicrotome EM UC7 (Leica Microsystems, Welzlar, Germany). Ultra-thin sections were collected on grids and stained with uranyl acetate and lead citrate. The samples were examined at 80 kV under a transmission electron microscope JEM-1400Flash (JEOL, Tokyo, Japan). To enumerate intact *Salmonella* within macrophages, images of ~30 infected macrophages were randomly obtained, the proportion in over 400 cells was analyzed on ImageJ.

Hydrogen peroxide sensitive GFP reporter—To visualize oxidative stress of bacteria during neutrophil phagocytosis or efferocytosis, we used a plasmid (pNB23) carrying the *katG* promoter cloned in front of a promoter-less *gfp* gene (Burton et al., 2014). To confirm ROS-dependent GFP synthesis, 5×10^7 cfu of S. Typhimurium carrying pNB23, a plasmid encoding mCherry, were incubated (37°C for 30 minutes) in the presence or absence of 100 μM hydrogen peroxide. After the incubation, cells were washed, fixed in 4% paraformaldehyde and then GFP expression visualized by fluorescence microscopy.

To visualize GFP synthesis during phagocytosis, 2×10^5 primary murine neutrophils were infected with 2×10^6 cfu of S. Typhimurium (pNB23) (MOI=10) in RPMI1640 medium supplemented with 15% fetal bovine serum (FBS), GlutaMAX™ supplement, and 25 mM HEPES (37°C, 5% CO_2). 2 hours after infection, infected neutrophils were washed by PBS and fixed in 4% paraformaldehyde.

To study efferocytosis, 23 hours after infection with S. Typhimurium (pNB23), RAW264.7 cells were incubated with 10% normal murine serum (NMS) for 30 minutes in (37°C, 5% CO_2) and then collected and counted. 4×10^5 infected RAW264.7 cells and 2×10^5 primary murine neutrophils were added to a coverslip in a 24-well plate, and neutrophil efferocytosis was allowed to proceed for 2 hours (37°C, 5% CO_2). Cells were then fixed in 4% paraformaldehyde. Neutrophils and nuclear morphology were visualized by anti-Ly6-G antibody and Hoechst 33342 DNA staining, respectively.

Quantitative real-time polymerase-chain reaction (qPCR)—To quantify oxidative stress in *S.* Typhimurium during neutrophil phagocytosis or neutrophil efferocytosis, transcripts of the oxidative stress inducible genes *katG* and *oxyS* were quantified by qPCR. To detect expression of *katG* and *oxyS* genes after *S.* Typhimurium exposure to hydrogen peroxide, 5×10^7 cfu of *S.* Typhimurium were incubated with different concentrations of

hydrogen peroxide at 37°C for 30 minutes. After the incubation, cells were washed, harvested by centrifugation and RNA was extracted using TRI Reagent® (Molecular Research Center).

To detect expression of *katG* and *oxyS* genes during neutrophil phagocytosis, 1×10^6 primary murine neutrophils were infected with 1×10^7 cfu of opsonized *S.* Typhimurium in RPMI1640 medium supplemented with 15% fetal bovine serum (FBS), GlutaMAX™, and 25mM HEPES (37°C, 5% CO_2). At 0, 0.5, and 2 hours after infection, infected neutrophils were washed by PBS and RNA extracted using TRI Reagent®.

To detect expression of *katG* and *oxyS* genes during neutrophil efferocytosis, 6×10^5 RAW264.7 murine macrophage-like cells were infected with 6×10^6 cfu opsonized *S.* Typhimurium in 6 well plates (MOI =10) and treated as described in efferocytosis assays described above. 23 hours after infection, RAW264.7 cells were incubated with 10% normal murine serum (NMS) for 30 minutes (37°C, 5% CO_2) and cells were collected and counted. 1×10^6 infected RAW264.7 cells and 1×10^6 primary murine neutrophils were added to a well and incubated for 0, 0.5, 2 hours (37°C, 5% CO_2). After incubation, cells were harvested and total RNA was extracted using TRI Reagent® (Molecular Research Center).

Complementary DNA (cDNA) from each RNA sample was generated by reverse transcription PCR (RT-PCR). Transcript levels of *katG* and *oxyS* were determined using a ViiA7 Real –Time PCR System (Applied Biosystems) using SYBR Green PCR Master Mix (Applied biosystems). Primers are listed in Table S1. The 16S ribosomal RNA gene for normalization, and delta delta Ct was used to calculate fold-changes between groups.

Lactate dehydrogenase (LDH) release—To quantify cell death, LDH released from cells during *S.* Typhimurium or *B. abortus* infection was measured by CytoTox™ 96 NonRadioactive Cytotoxicity Assay kit (Promega) according to the manufacturer's instruction. Briefly, for *S.* Typhimurium, 5×10^4 RAW264.7 murine macrophage-like cells were infected with 5×10^5 opsonized bacteria (MOI=10) in a 96-well plate. For *B. abortus*, 2×10^5 BMDMs were infected with opsonized bacteria at the indicated MOIs in a 24-well plate. The plate was centrifuged at 250 μ g for 5 minutes and incubated (37°C, 5% CO_2) for 30 minutes to allow for uptake of bacteria. Extracellular *S.* Typhimurium and *B. abortus* were killed by 30-minute incubation with 100 μg/mL or 50 μg/mL gentamicin, respectively. The gentamicin concentration was then reduced to 10 μg/mL for *S.* Typhimurium or removed for *B. abortus* for the remainder of the experiment. 24 hours after infection, supernatants from each well were collected and the level of LDH release were determined following manufacturer instructions. Macrophage cell death was expressed as % of LDH released after cell lysis.

Quantification and Statistical analyses

Ratios (i.e. fold-change, competitive index and percentage values) were converted logarithmically prior to statistical analysis. All data are expressed as the geometric mean ± standard error. ANOVA was used for animal experiments and multiple comparisons and Student's *t*-tests was used for pairwise comparison. For quantification of data from transmission electron microscopy, counts were converted into binary numbers (Live = 1 and

Dead = 0) and analyzed using a Mann-Whitney test. $P < 0.05$ was considered significant. Statistical details of experiments, including exact value of N and what N represents, can be found in the figure legends.

Supplementary Material

Refer to Web version on PubMed Central for supplementary material.

ACKNOWLEDGEMENTS

We thank Dr. Matthias Mack for kindly providing anti-CCR2 antibody. H.H. was supported by NIH award AI143929, UC Davis Innovative Development Award, a Takeda Science Foundation grant, a Daiichi Sankyo Foundation fellowship and JSPS KAKENHI Grant Number JP21K07027. T.W. was supported by NIH award AI126080. L.F.Z. was supported by NIH Grant AI36309. Work in A.J.B.'s laboratory was supported by USDA/NIFA award 2015-67015-22930 and NIH awards AI044170, AI096528, AI112445, AI112949 and AI146432. Work in R.M.T.'s laboratory was supported by NIH awards AI143253, AI149632, AI112949, AI089078 and AI109799.

REFERENCES

Atluri VL, Xavier MN, de Jong MF, den Hartigh AB, and Tsolis RM (2011). Interactions of the human pathogenic Brucella species with their hosts. Annu Rev Microbiol 65, 523–541. [PubMed: 21939378]

Barquero-Calvo E, Chaves-Olarte E, Weiss DS, Guzman-Verri C, Chacon-Diaz C, Rucavado A, Moriyon I, and Moreno E (2007). Brucella abortus uses a stealthy strategy to avoid activation of the innate immune system during the onset of infection. PLoS One 2, e631. [PubMed: 17637846]

Bravo D, Silva C, Carter JA, Hoare A, Alvarez SA, Blondel CJ, Zaldivar M, Valvano MA, and Contreras I (2008). Growth-phase regulation of lipopolysaccharide O-antigen chain length influences serum resistance in serovars of Salmonella. J Med Microbiol 57, 938–946. [PubMed: 18628492]

Burton NA, Schurmann N, Casse O, Steeb AK, Claudi B, Zankl J, Schmidt A, and Bumann D (2014). Disparate impact of oxidative host defenses determines the fate of Salmonella during systemic infection in mice. Cell Host Microbe 15, 72–83. [PubMed: 24439899]

Conlan JW (1996). Neutrophils prevent extracellular colonization of the liver microvasculature by Salmonella typhimurium. Infect Immun 64, 1043–1047. [PubMed: 8641757]

Cookson BT, and Brennan MA (2001). Pro-inflammatory programmed cell death. Trends Microbiol 9, 113–114. [PubMed: 11303500]

Cummings LA, Wilkerson WD, Bergsbaken T, and Cookson BT (2006). In vivo, fliC expression by Salmonella enterica serovar Typhimurium is heterogeneous, regulated by ClpX, and anatomically restricted. Mol Microbiol 61, 795–809. [PubMed: 16803592]

de Barsy M, Jamet A, Filopon D, Nicolas C, Laloux G, Rual JF, Muller A, Twizere JC, Nkengfac B, Vandenhaute J, et al. (2011). Identification of a Brucella spp. secreted effector specifically interacting with human small GTPase Rab2. Cell Microbiol 13, 1044–1058. [PubMed: 21501366]

de Jong MF, Sun YH, den Hartigh AB, van Dijl JM, and Tsolis RM (2008). Identification of VceA and VceC, two members of the VjbR regulon that are translocated into macrophages by the Brucella type IV secretion system. Mol Microbiol 70, 1378–1396. [PubMed: 19019140]

Dunlap NE, Benjamin WH Jr., Berry AK, Eldridge JH, and Briles DE (1992). A 'safe-site' for Salmonella typhimurium is within splenic polymorphonuclear cells. Microb Pathog 13, 181–190. [PubMed: 1291841]

Fadok VA, de Cathelineau A, Daleke DL, Henson PM, and Bratton DL (2001). Loss of phospholipid asymmetry and surface exposure of phosphatidylserine is required for phagocytosis of apoptotic cells by macrophages and fibroblasts. J Biol Chem 276, 1071–1077. [PubMed: 10986279]

Fink SL, and Cookson BT (2019). Pillars Article: Caspase-1-dependent pore formation during pyroptosis leads to osmotic lysis of infected host macrophages. Cell Microbiol. 2006. 8: 1812–1825.J Immunol 202, 1913–1926.

Franchi L, Amer A, Body-Malapel M, Kanneganti TD, Ozoren N, Jagirdar R, Inohara N, Vandenabeele P, Bertin J, Coyle A, et al. (2006). Cytosolic flagellin requires Ipaf for activation of caspase-1 and interleukin 1beta in salmonella-infected macrophages. Nat Immunol 7, 576–582. [PubMed: 16648852]

Grant AJ, Morgan FJ, McKinley TJ, Foster GL, Maskell DJ, and Mastroeni P (2012). Attenuated Salmonella Typhimurium lacking the pathogenicity island-2 type 3 secretion system grow to high bacterial numbers inside phagocytes in mice. PLoS Pathog 8, e1003070. [PubMed: 23236281]

Hensel M, Shea JE, Gleeson C, Jones MD, Dalton E, and Holden DW (1995). Simultaneous identification of bacterial virulence genes by negative selection. Science 269, 400–403. [PubMed: 7618105]

Herb M, Gluschko A, and Schramm M (2021). Reactive Oxygen Species: Not Omnipresent but Important in Many Locations. Front Cell Dev Biol 9, 716406. [PubMed: 34557488]

Hiyoshi H, Wangdi T, Lock G, Saechao C, Raffatellu M, Cobb BA, and Bäumler AJ (2018). Mechanisms to evade the phagocyte respiratory burst arose by convergent evolution in typhoidal Salmonella serovars. Cell Reports 22, 1787–1797. [PubMed: 29444431]

Hong PC, Tsolis RM, and Ficht TA (2000). Identification of genes required for chronic persistence of Brucella abortus in mice. Infect Immun 68, 4102–4107. [PubMed: 10858227]

Ikari N, Sakai Y, Hitomi Y, and Fujii S (1983). New synthetic inhibitor to the alternative complement pathway. Immunology 49, 685–691. [PubMed: 6553561]

Jorgensen I, Zhang Y, Krantz BA, and Miao EA (2016). Pyroptosis triggers pore-induced intracellular traps (PITs) that capture bacteria and lead to their clearance by efferocytosis. J Exp Med 213, 2113–2128. [PubMed: 27573815]

Knodler LA, Nair V, and Steele-Mortimer O (2014). Quantitative assessment of cytosolic Salmonella in epithelial cells. PLoS One 9, e84681. [PubMed: 24400108]

LaRock DL, Chaudhary A, and Miller SI (2015). Salmonellae interactions with host processes. Nat Rev Microbiol 13, 191–205. [PubMed: 25749450]

Li P, Tian M, Bao Y, Hu H, Liu J, Yin Y, Ding C, Wang S, and Yu S (2017). Brucella Rough Mutant Induce Macrophage Death via Activating IRE1alpha Pathway of Endoplasmic Reticulum Stress by Enhanced T4SS Secretion. Front Cell Infect Microbiol 7, 422. [PubMed: 29021973]

Mack M, Cihak J, Simonis C, Luckow B, Proudfoot AE, Plachy J, Bruhl H, Frink M, Anders HJ, Vielhauer V, et al. (2001). Expression and characterization of the chemokine receptors CCR2 and CCR5 in mice. J Immunol 166, 4697–4704. [PubMed: 11254730]

Marchesini MI, Herrmann CK, Salcedo SP, Gorvel JP, and Comerci DJ (2011). In search of Brucella abortus type IV secretion substrates: screening and identification of four proteins translocated into host cells through VirB system. Cell Microbiol 13, 1261–1274. [PubMed: 21707904]

Matsuda S, Haneda T, Saito H, Miki T, and Okada N (2019). Salmonella enterica Effectors SifA, SpvB, SseF, SseJ, and SteA Contribute to Type III Secretion System 1-Independent Inflammation in a Streptomycin-Pretreated Mouse Model of Colitis. Infect Immun 87.

Meunier E, and Broz P (2015). Quantification of Cytosolic vs. Vacuolar Salmonella in Primary Macrophages by Differential Permeabilization. J Vis Exp, e52960. [PubMed: 26274778]

Miao EA, Alpuche-Aranda CM, Dors M, Clark AE, Bader MW, Miller SI, and Aderem A (2006). Cytoplasmic flagellin activates caspase-1 and secretion of interleukin 1beta via Ipaf. Nat Immunol 7, 569–575. [PubMed: 16648853]

Monack DM, Raupach B, Hromockyj AE, and Falkow S (1996). Salmonella typhimurium invasion induces apoptosis in infected macrophages. Proc Natl Acad Sci U S A 93, 9833–9838. [PubMed: 8790417]

Myeni S, Child R, Ng TW, Kupko JJ 3rd, Wehrly TD, Porcella SF, Knodler LA, and Celli J (2013). Brucella modulates secretory trafficking via multiple type IV secretion effector proteins. PLoS Pathog 9, e1003556. [PubMed: 23950720]

Pei J, Wu Q, Kahl-McDonagh M, and Ficht TA (2008). Cytotoxicity in macrophages infected with rough Brucella mutants is type IV secretion system dependent. Infect Immun 76, 30–37. [PubMed: 17938217]

Richter-Dahlfors A, Buchan AM, and Finlay BB (1997). Murine salmonellosis studied by confocal microscopy: Salmonella typhimurium resides intracellularly inside macrophages and exerts a cytotoxic effect on phagocytes in vivo. J Exp Med 186, 569–580. [PubMed: 9254655]

Rolan HG, and Tsolis RM (2007). Mice lacking components of adaptive immunity show increased Brucella abortus virB mutant colonization. Infect Immun 75, 2965–2973. [PubMed: 17420243]

Stauffer W, Sheng H, and Lim HN (2018). EzColocalization: An ImageJ plugin for visualizing and measuring colocalization in cells and organisms. Sci Rep 8, 15764. [PubMed: 30361629]

Sun YH, Rolan HG, and Tsolis RM (2007). Injection of flagellin into the host cell cytosol by Salmonella enterica serotype typhimurium. J Biol Chem.

Terwagne M, Ferooz J, Rolan HG, Sun YH, Atluri V, Xavier MN, Franchi L, Nunez G, Legrand T, Flavell RA, et al. (2013). Innate immune recognition of flagellin limits systemic persistence of Brucella. Cell Microbiol 15, 942–960. [PubMed: 23227931]

Thurston TL, Wandel MP, von Muhlinen N, Foeglein A, and Randow F (2012). Galectin 8 targets damaged vesicles for autophagy to defend cells against bacterial invasion. Nature 482, 414–418. [PubMed: 22246324]

Tian M, Yin Y, Lian Z, Li Z, Song M, Hu H, Guan X, Ding C, Wang S, Li T, et al. (2020). A rough Brucella mutant induced macrophage death depends on secretion activity of T4SS, but not on cellular Txnip- and Caspase-2-mediated signaling pathway. Vet Microbiol 244, 108648. [PubMed: 32402333]

van der Velden AW, Lindgren SW, Worley MJ, and Heffron F (2000). Salmonella pathogenicity island 1-independent induction of apoptosis in infected macrophages by Salmonella enterica serotype typhimurium. Infect Immun 68, 5702–5709. [PubMed: 10992474]

Vance RE, Isberg RR, and Portnoy DA (2009). Patterns of pathogenesis: discrimination of pathogenic and nonpathogenic microbes by the innate immune system. Cell Host Microbe 6, 10–21. [PubMed: 19616762]

Vazquez-Torres A, Xu Y, Jones-Carson J, Holden DW, Lucia SM, Dinauer MC, Mastroeni P, and Fang FC (2000). Salmonella Pathogenicity Island 2-Dependent Evasion of the Phagocyte NADPH Oxidase. Science 287, 1655–1658. [PubMed: 10698741]

Wangdi T, Lee C-Y, Spees AM, Yu C, Kingsbury DD, Winter SE, Hastey CJ, Wilson RP, Heinrich V, and Bäumler AJ (2014). The Vi capsular polysaccharide enables Salmonella enterica serovar Typhi to evade microbe-guided neutrophil chemotaxis. PLOS Pathogens 10, e1004306. [PubMed: 25101794]

Zhang X, Majlessi L, Deriaud E, Leclerc C, and Lo-Man R (2009). Coactivation of Syk kinase and MyD88 adaptor protein pathways by bacteria promotes regulatory properties of neutrophils. Immunity 31, 761–771. [PubMed: 19913447]

Highlights

- *Salmonella* T3SS-2 functions in evading neutrophil-mediated host control
- T3SS-2 impairs endo-lysosomal integrity of the *Salmonella*-containing vacuole (SCV)
- SCV perforation triggers a complement dependent find-me signal for efferocytosis
- Efferocytosis shelters *Salmonella* entrapped in PITs from killing by neutrophils

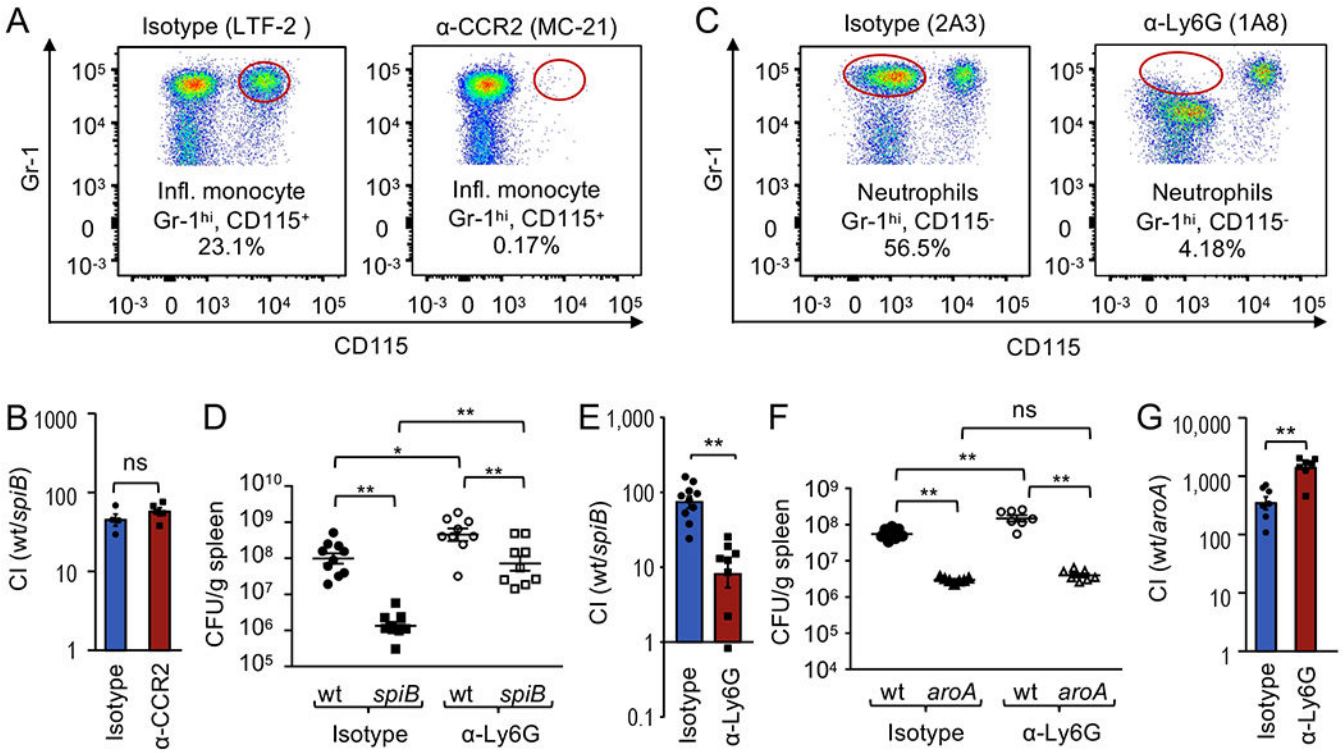

Figure 1: T3SS-2 enables *STm* to evade neutrophil-mediated host defenses *in vivo*.

(A and B) Mice injected with anti-CCR2 (*α*-CCR2) monoclonal antibody (clone MC-21) or an isotype control (clone LTF-2) were infected intraperitoneally with a 1:1 mixture of the *STm* wild type (wt) and an isogenic *spiB* mutant. (A) The fraction of inflammatory monocytes (Gr-1^{hi} CD115^{+} cells) in single cell suspensions of splenic CD11b^{+}, CD3^{-}, NK1.1^{-}, B220^{-} cells was determined by flow cytometry. (B) The competitive index (CI, ratio of wt and *spiB* mutant) recovered from the spleen two days after infection was determined. (C-G) Mice were injected with anti-Ly6G (*α*-Ly6G) monoclonal antibody (clone 1A8) or an isotype control (clone 2A3). (C-E) Mice were injected intraperitoneally with a 1:1 mixture of the *STm* wild type (wt) and an isogenic *spiB* mutant (*spiB*). (C) The fraction of neutrophils (Gr-1^{hi}, CD115^{-} cells) in single cell suspensions of splenic CD11b^{+}, CD3^{-}, NK1.1^{-}, B220^{-} cells was determined by flow cytometry. (D) The graph shows colony-forming units (cfu) of wt and *spiB* mutant recovered from the spleen two days after infection. (E) The CI recovered from the spleen was determined. (F-G) Mice were injected intraperitoneally with a 1:1 mixture of the *STm* wild type (wt) and an isogenic *aroA* mutant (*aroA*). (F) The graph shows cfu of wt and *aroA* mutant recovered from the spleen two days after infection. (G) The CI recovered from the spleen was determined. (A-G) Each symbol in panel B and panels D through G represents data from one animal. Group sizes (*N*) are indicated by the number of symbols. Panels A and C show data from one representative animal. *, $P < 0.05$; **, $P < 0.01$: ns, $P > 0.05$.

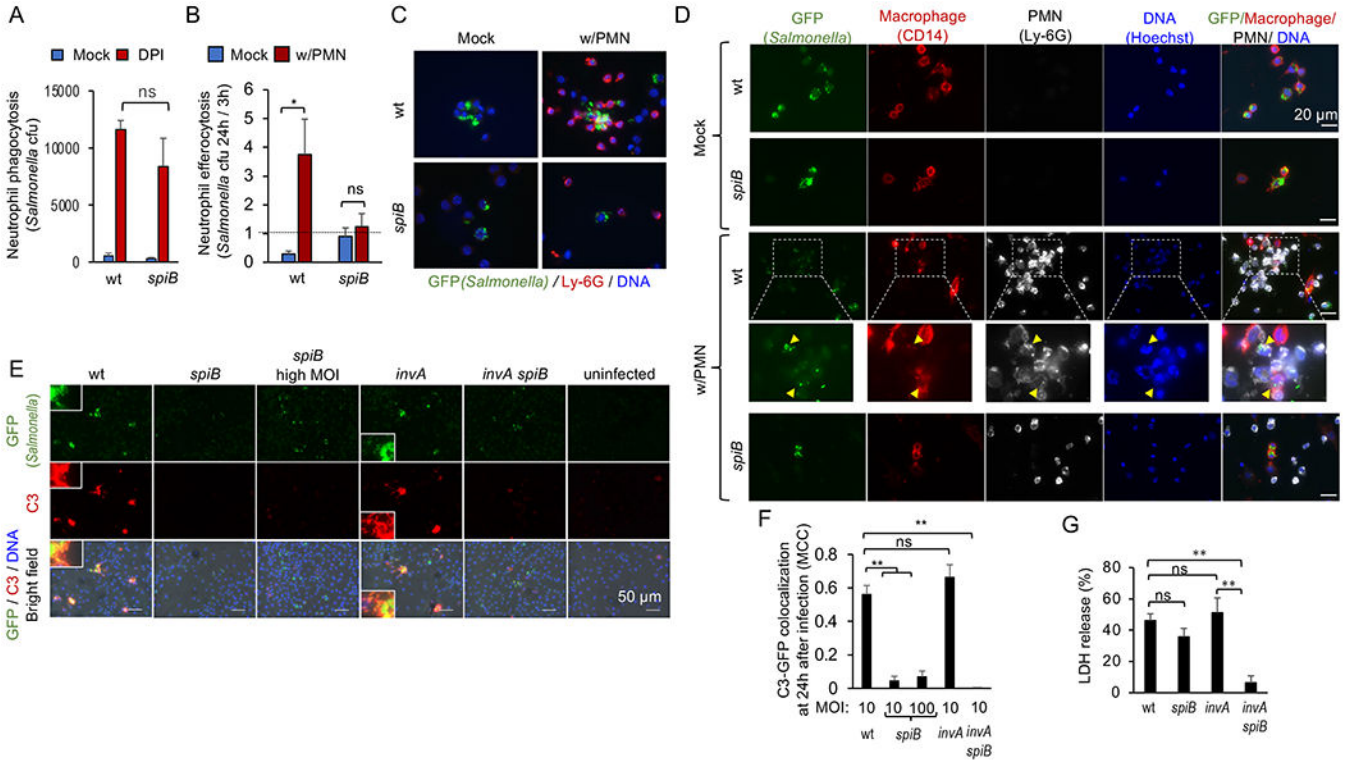

Figure 2: T3SS-2 triggers C3 deposition on bacteria entrapped in PITs.

(A) Primary murine neutrophils were either mock-treated (Mock) or treated with 5μM diphenyleneiodonium chloride (DPI) and subsequently infected with the *STm* wild type (wt) or a *spiB* mutant. Two hours after infection, intracellular bacteria were recovered from neutrophils and colony-forming units (cfu) enumerated. (B) Murine macrophage-like RAW264.7 cells (macrophages) were infected with the indicated *STm* strains. 23 hours later, cells were either mock treated (mock), or primary murine neutrophils were added (w/PMN). The graph shows the change in cfu between 3 hours and 21 hours after the addition of neutrophils. (C-G) Macrophages were infected with the indicated *STm* strains expressing green fluorescence protein (GFP, green fluorescence). (C and D) 23 hours after infection of macrophages, cells were either mock treated (mock), or primary murine neutrophils were added (w/PMN). (C) Neutrophils were detected with a Ly6G-specific monoclonal antibody (red fluorescence) and cells were counter stained with a nuclear stain (blue fluorescence). (D) Neutrophils were detected with a Ly6G-specific monoclonal antibody (white fluorescence), macrophages were detected with a CD14-specific monoclonal antibody (red fluorescence) and cells were counter stained with a nuclear stain (blue fluorescence). (E and F) 24 hours after infection of macrophages, normal mouse serum was added and samples were analyzed 30 minutes later. Complement component 3 (C3) was detected with anti-mouse C3 antibody (red fluorescence). (E) Representative images. (F) The Manders' Colocalization Coefficient (MCC) for C3 staining and GFP staining was determined by image analysis of 20 microscopic fields per group. (G) 24 hours after infection of macrophages, cell death was assessed by measuring lactate dehydrogenase (LDH) release. Data are shown as % LDH release observed in mock-infected macrophages.

(A, B, F, and G) Data represent geometric means from three ($N = 3$) independent biological repeats + standard error. **, $P < 0.01$: ns, $P > 0.05$.

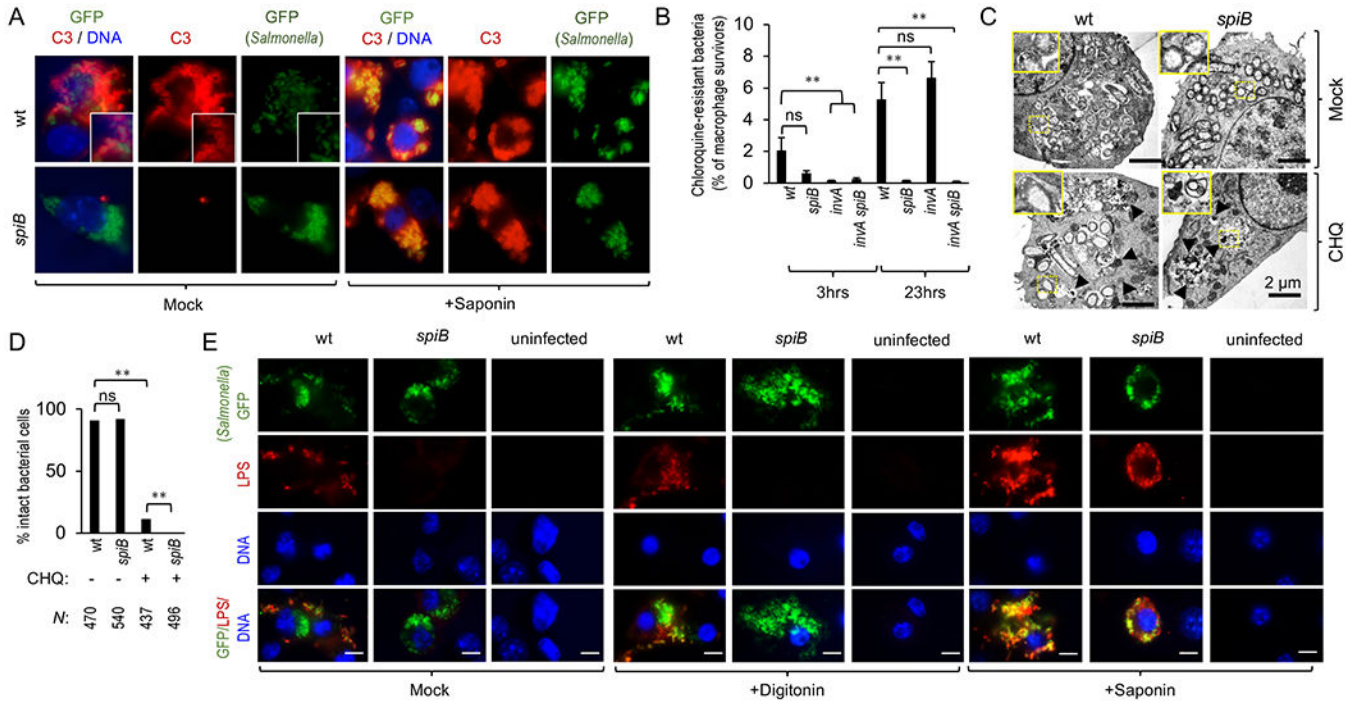

Figure 3: T3SS-2-mediated perforation of the SCV is required for C3 deposition on bacteria entrapped in PITs.

(A and E) Macrophages were infected with the indicated *STm* strains expressing green fluorescence protein (GFP, green fluorescence). (A) 23 hours after infection, saponin was added or cells remained untreated (mock). Normal mouse serum was added and murine complement component 3 (C3) was detected with anti-murine C3 antibody (red fluorescence). Cells were counter stained with nuclear stain (blue fluorescence). (B-D) Macrophages infected with the indicated *STm* strains were mock treated or treated with 500 µM chloroquine (CHQ) for 2 hours. (B) Colony-forming units were determined at the indicated time points after infection. The graph shows chloroquine-resistant cfu as percentage of total cfu recovered from mock-treated cells. Data represent geometric means from four ($N = 4$) independent biological repeats + standard error. (C and D) 23 hours after infection macrophages were analyzed by transmission electron microscopy. (C) Representative images. Arrow heads point to dead bacteria. (D) Intact bacteria as a fraction of the total bacterial count (*N*). (E) 24 hours after infection digitonin or saponin were added, or cells were mock treated. An anti-O12 antiserum (LPS, red fluorescence) was added and cells were counter stained with Hoechst nuclear stain (DNA, blue fluorescence). **, $P < 0.01$: ns, $P > 0.05$.

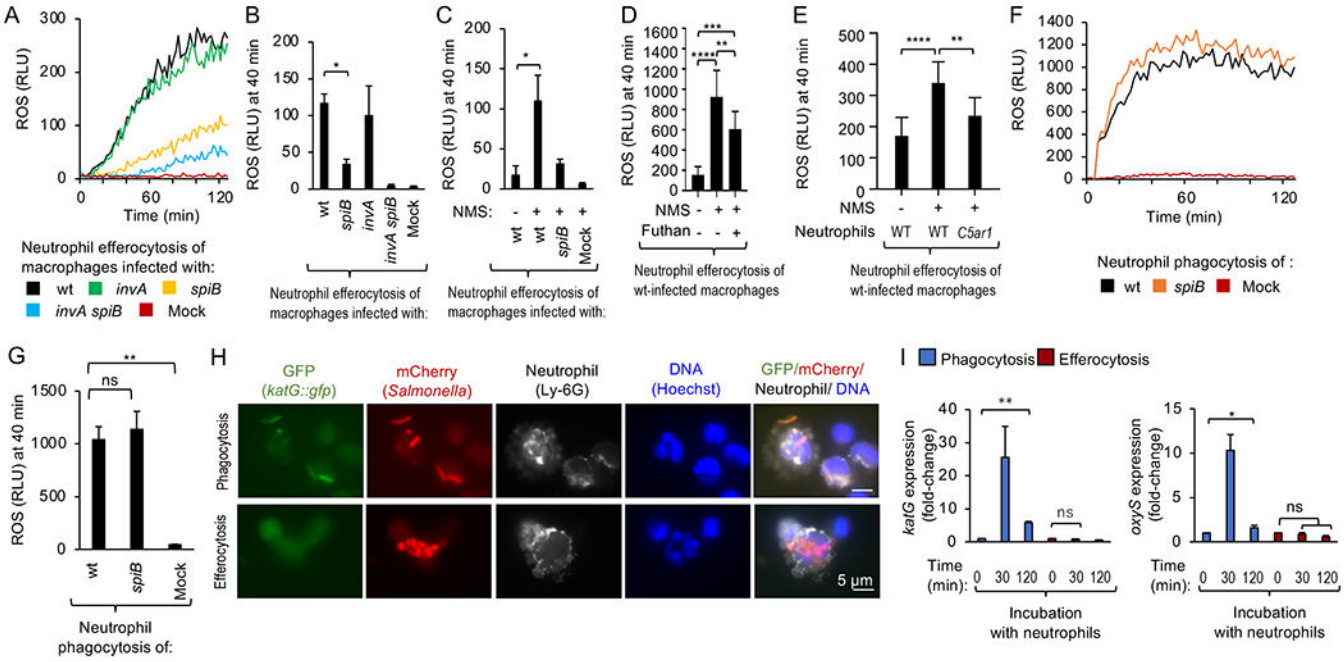

Figure 4: Neutrophil efferocytosis of bacteria entrapped in PITs shelters *STm* from exposure to ROS.

(A-E) Murine macrophage-like RAW264.7 cells (macrophages) were infected with the indicated *STm* strains. RLU, relative luminescence units. (A and B) After 24 hours, normal mouse serum was added to infected macrophages. Neutrophils were added 30 minutes later. Production of reactive oxygen species (ROS) during efferocytosis was monitored using chemiluminescence. (A) Representative experiment showing generation of chemiluminescence over time. (B) The graph shows the average chemiluminescence from four ($N = 4$) independent experiments at the indicated time point after adding neutrophils. (C-E) After 24 hours, normal mouse serum (NMS: +) (C and E) or mouse serum incubated with Futhan (Futhan: +) (D) was added or cells remained untreated (NMS: −) and neutrophils from C57BL/6J mice (C and D) or *C5aR1*-deficient mice (E) were added 30 minutes later. The graph shows the average chemiluminescence from three independent experiments ($N = 3$) at the indicated time point after adding neutrophils. (F and G) Primary murine neutrophils were mock infected or infected with indicated opsonized *STm* strains. ROS production was monitored using chemiluminescence. (F) Representative experiment. (G) Average chemiluminescence from four independent experiments ($N = 4$) at the indicated time point after infecting neutrophils. (H) For phagocytosis, neutrophils (Ly6G, white fluorescence) were infected for two hours with an opsonized *STm* strain constitutively synthesizing mCherry (red fluorescence) and expressing *gfp* under control of the *katG* promoter (P_{katG}::*gfp*) (GFP, green fluorescence) and then counter stained with Hoechst (DNA, blue fluorescence). For efferocytosis, macrophages infected for 24 hours with aforementioned *STm* strain were treated with normal mouse serum, followed 30 minutes later by the addition of primary murine neutrophils. Two hours later, cells were counter stained with Hoechst (DNA, blue fluorescence). (I) Transcript levels of hydrogen peroxide-inducible genes (*katG* and *oxyR*) were determined at the indicated time points after adding neutrophils to *STm* (phagocytosis) or to *STm*-infected macrophages (efferocytosis)

using quantitative real-time PCR. Data represent geometric means from three independent experiments ($N = 3$) + standard error. *, $P < 0.05$; **, $P < 0.01$: ns, $P > 0.05$.

KEY RESOURCES TABLE

REAGENT or RESOURCE	SOURCE	IDENTIFIER
Antibodies		
*In Vivo*MAb anti-mouse Ly-6G (1A8)	Bio X Cell	Cat#BE0075-1; RRID:AB_1107721
*In Vivo*MAb rat IgG2a isotype control, anti-trinitrophenol (2A3)	Bio X Cell	Cat#BE0089; RRID:AB_1107769
*In Vivo*MAb rat IgG2b isotype control, anti-keyhole limpet hemocyanin (LTF-2)	Bio X Cell	Cat#BE0090; RRID:AB_1107780
Anti-CCR2 antibody (MC-21)	(Mack et al., 2001)	Cat#CCR2 (MC21); RRID:AB_2314128
Salmonella O Antiserum Factor 12	Becton Dickinson	Cat#227791
Goat IgG Fraction to Mouse Complement C3	MP Biomedicals	Cat#ICN55463; RRID:AB_2334481
Alexa Fluor 568 donkey anti-rabbit IgG (H+L)	Invitrogen	Cat#A10042; RRID:AB_2534017
Alexa Fluor 568 donkey anti-goat IgG (H+L)	Invitrogen	Cat#A-11057; RRID:AB_142581
Alexa Fluor 488 donkey anti-mouse IgG (H+L)	Invitrogen	Cat#A-21202; RRID:AB_141607
PE anti-mouse CD3 (17A2)	BioLegend	Cat#100206; RRID:AB_312663
PE anti-mouse/human CD45R/B220 (RA3-6B2)	BioLegend	Cat#103207; RRID:AB_312992
PE anti-mouse NK-1.1 (PK136)	BioLegend	Cat#108708; RRID:AB_313395
PE/Cy7 anti-mouse/human CD11b (M1/70)	BioLegend	Cat#101215; RRID:AB_312798
Brilliant Violet 421 anti-mouse CD115 (CSF-1R) (AFS98)	BioLegend	Cat#135513; RRID:AB_2562667
APC Ly-6G/Ly-6C Monoclonal Antibody (RB6-8C5)	eBioscience	Cat#17-5931-82; RRID:AB_469476
Alexa Fluor® 647 anti-mouse Ly-6G Antibody	BioLegend	Cat#127609; RRID:AB_1134162
Biotin anti-mouse CD14 Antibody	BioLegend	Cat#123305; RRID:AB_940586
Rhodamine (TRITC) Streptavidin	Jackson Immuno Research Laboratories	Cat#016-020-084; RRID:AB_2337237
Bacterial and Virus Strains		
For strains used in this study see Table S1	see Table S1	see Table S1
Biological Samples		
For plasmids used in this study see Table S1	see Table S1	see Table S1
Chemicals, Peptides, and Recombinant Proteins		
Digitonin	Sigma-Aldrich	Cat#D141
Saponin	Sigma-Aldrich	Cat#S4521
Diphenyleneiodonium chloride (DPI)	Sigma-Aldrich	Cat#D2926
Chloroquine diphosphate salt	Sigma-Aldrich	Cat#C6628
Hoechst 33342	Invitrogen	Cat#H3570
ProLong™ Diamond Antifade Mountant	Invitrogen	Cat#P36965
Hydrogen peroxide	EMD	Cat#HX0635
Luminol	Sigma-Aldrich	Cat#123072
BD Cytofix™ Fixation buffer	Becton Dickinson	Cat#554655

REAGENT or RESOURCE	SOURCE	IDENTIFIER
Live/Dead Fixable Aqua Dead Cell Stain kit	Invitrogen	Cat#L34957
FUT-175 (Futhan, 6-amidino-2-naphthyl *p*-guanidinobenzoate dimethanesulfonate)	BD Biosciences	Cat#552035; AB_2868956
Xfect™ Transfection Reagent	Clontech	Cat#631317
Critical Commercial Assays		
TRI-reagent	Molecular Research Center	Cat#TR118
DNA-free DNA Removal Kit	Applied Biosystems	Cat#AM1906
SYBR Green PCR Master Mix	Applied Biosystems	Cat#4309155
Zymoclean Gel DNA Recovery Kit	Zymo Research	Cat#D4001
QIAprep Spin Miniprep Kit	Qiagen	Cat#27106
Experimental Models: Cell lines		
Mouse macrophage-like cell: RAW264.7	ATCC	Cat#TIB-71, RRID:CVCL_0493
Experimental Models: Organisms/Strains		
Mouse: C57BL/6J	Jackson Labs	Cat#JAX:000664, RRID:IMSR_JAX:000664
Mouse: B6.129S4(C)-*C5ar1*^{tm1Cge}/BaoluJ	Jackson Labs	Cat#JAX:033903, RRID:IMSR_JAX:033903
Oligonucleotides		
For qRT-PCR primers used in this study see Table S1	see Table S1	see Table S1
Software and Algorithms		
Prism v8.0	GraphPad	http://www.graphpad.com
Microsoft Excel for Mac	Microsoft	N/A
MacVector v15.5.4	MacVector	https://macvector.com/
ImageJ (Fiji)	NIH	https://fiji.sc/